Eur. Phys. J. A **11**, 79–85 (2001)

THE EUROPEAN PHYSICAL JOURNAL A

Spectral analysis of ^{208}Pb muonic atom

F.-Z. Ighezou[1], R.J. Lombard[2,a], and J. Mareš[3,b]

[1] Université des Sciences et de la Technologie Houari Boumédienne, BP 32 El-Alia, 16111 Bab Ezzouar, Alger, Algeria
[2] Groupe de Physique Théorique, Institut de Physique Nucléaire, 91406 Orsay Cedex, France
[3] Nuclear Physics Institute, 250 68 Řež, Czech Republic

Received: 18 December 2000 / Revised version: 29 March 2001
Communicated by P. Schuck

Abstract. We have applied to the ^{208}Pb muonic atom a series of recurrence relations relating the moments of the ground-state density and the energy differences between the $1s$ level and the states of the *yrast* line. The large amount of precise experimental data and the electromagnetic character of the interaction allow a detailed test of the method for determining the ground-state density and reconstructing the local equivalent potential. Though the present work is limited to the study of the efficiency for a given trial density, it results in a semi-quantitative analysis with an accuracy better than 1%.

PACS. 36.10.Gv Mesonic atoms and molecules, hyperonic atoms and molecules – 03.65.Ge Solutions of wave equations: bound states – 02.30.Zz Inverse problems

1 Introduction

A series of recurrence relations connecting the energy of the *yrast* levels to the moments of the ground-state density was developed in the framework of two-body non-relativistic quantum mechanics [1,2]. These expressions were derived by generalizing the Bertlmann-Martin inequality [3] between the lowest dipole excitation energy and the rms radius of the ground state. They are valid for local potentials but inclusion of non-locality can also be handled in some cases [4]. An application of the method to Λ-hypernuclei yielded the bulk features of the Λ wave function inside the nucleus. Since the spectroscopic data of muonic atoms are incomparably more accurate, their analysis represents a much more severe test of the method.

Muonic atoms, widely studied in the seventies, provide us with accurate data on energy levels [5]. Due to the known electromagnetic character of the interaction, a careful analysis of the spectra was achieved. Fitting the atomic spectra together with the electron data brought valuable information about the nuclear charge distribution. A useful review of the field is given by Barrett and Jackson [6].

The muon actually obeys a Dirac equation and, moreover, quantum electrodynamic corrections have also to be included, so that the reference to a Schrödinger equation may sound inappropriate. However, the method we are advocating reaches an accuracy of no better than 0.5%. At this level, according to the values quoted for ^{208}Pb [6], the main effects come from the extended nuclear-charge distribution. Thus, in spite of limitations, it is tempting to apply our relations to the case of muonic atoms to try to get a muonic ground-state wave function in a model independent way. The subsequent step consists in reconstructing an equivalent local potential and in its comparison with the potential calculated from the charge distribution.

It is obvious that the present method can be tested on any local potential by solving the Schrödinger equation and comparing the moments of the ground-state density with the results of the recurrence relations, as was done for few typical examples in ref. [4]. From this study we know the range of accuracy that might be expected. Nevertheless, it is challenging to check the method on real, physical data. Moreover, the possibility of reconstructing the potential has so far not been investigated. Thus, the aim of the present work is to make such analysis in the case of the ^{208}Pb muonic atom. It gives us an opportunity to understand the contribution of the method to the so-called inverse problem [7].

The paper is organized as follows. In sect. 2, the series of recurrence relations is briefly recalled. The data analysis is given in sect. 3, and conclusions are drawn in sect. 4.

2 The recurrence relations

The derivation of the series of recurrence relations that we are using, together with its validity conditions, was given in previous papers [1,2]. Therefore, we only quote here

[a] e-mail: Lombard@ipno.in2p3.fr
[b] e-mail: mares@ujf.cas.cz

the main steps. The starting point is a series of inequalities obtained from the sum rule linear in energy of the operator $Q_{\ell,0}(\mathbf{r}) = r^\ell Y_{\ell,0}(\theta,\phi)$:

$$(E_{1\ell} - E_{1s}) \sum_n |\langle 0|Q_{\ell,0}|n\ell\rangle|^2 \leq \sum_n (E_{n\ell} - E_{1s})|\langle 0|Q_{\ell,0}|n\ell\rangle|^2 \ . \quad (1)$$

It leads to

$$\langle r^{2\ell}\rangle \ \leq \ \frac{\hbar^2}{2\mu}\ell(2\ell+1)\frac{\langle r^{2\ell-2}\rangle}{(E_{1\ell} - E_{1s})} \ , \quad (2)$$

which can be converted into equalities by introducing a correction factor

$$\langle r^{2\ell}\rangle = \frac{\hbar^2}{2\mu}\ell(2\ell+1)\frac{\langle r^{2\ell-2}\rangle}{(E_{1\ell} - E_{1s})}\Big[1 - \frac{\ell}{2(\ell+1)}C(\ell)\Big]. \quad (3)$$

In these expressions $\langle r^k\rangle$ is the k-th moment of the ground-state density,

$$\langle r^k\rangle \ = \int |\Phi_{1s}(\mathbf{r})|^2 \ r^k \ \mathrm{d}^3 r \ , \quad (4)$$

where Φ_{1s} is the ground-state wave function; μ is the reduced mass, $E_{1\ell}$ is the lowest eigenvalue of angular momentum ℓ. Thus, the levels entering (2) and (3) are those of the *yrast* line. Note that we are not using the spectroscopic notation of atomic physics. Here, $n\ell$ denotes the n-th level of angular momentum ℓ; the number of nodes of the wave function is given by $n-1$.

In the case of a particle with non-zero spin, the spin-orbit splitting must be taken into account. However, the operators used to generate relations (3) excite the spin-orbit partners with an equal strength, except for peculiar situations when one of the partners is close to the continuum threshold. Consequently, as shown in [1], a weighted average has to be taken

$$E_{1\ell} = \frac{1}{(2\ell+1)}\Big[(\ell+1)E_{j=\ell+1/2} + \ell E_{j=\ell-1/2}\Big] \ . \quad (5)$$

The correction factors $C(\ell)$ depend on the potential. Thus, the usefulness of eq. (3) is clearly linked to the possibility of finding an expression for $C(\ell)$ valid for a large class of potentials. Otherwise $C(\ell)$ have to be calculated in each case with no advantage over the direct solution of the Schrödinger equation. It turns out that the form suggested by Bertlmann and Martin [3] is quite efficient for various potentials [2]. It is based on the results for the harmonic oscillator ($C(\ell) = 0, \forall\ell$) and the Coulomb point charge potential ($C(\ell) = 1, \forall\ell$), for which we know the exact result. It reads

$$C(\ell) = \left[\frac{E_{(\ell+1)s} + E_{1s} - 2E_{1\ell}}{E_{(\ell+1)s} - E_{1s}}\right]^2 \ . \quad (6)$$

Unfortunately, this form is not universal. Except for the two reference potentials, its application merely reduces eq. (3) to a collection of approximate relationships. However, as stated above, this approximation appears quite satisfactory in many cases [2]; for instance an accuracy better than 1% is reached for confining potentials [8]. This can be sufficient at a qualitative level but we may face situations in which it is desirable to deal with more accurate correction factors. This may happen, in particular, when one tries to reconstruct a potential (assumed unknown) from the *yrast* energy levels. It could then be necessary to proceed by iterations, taking eq. (6) as a first guess.

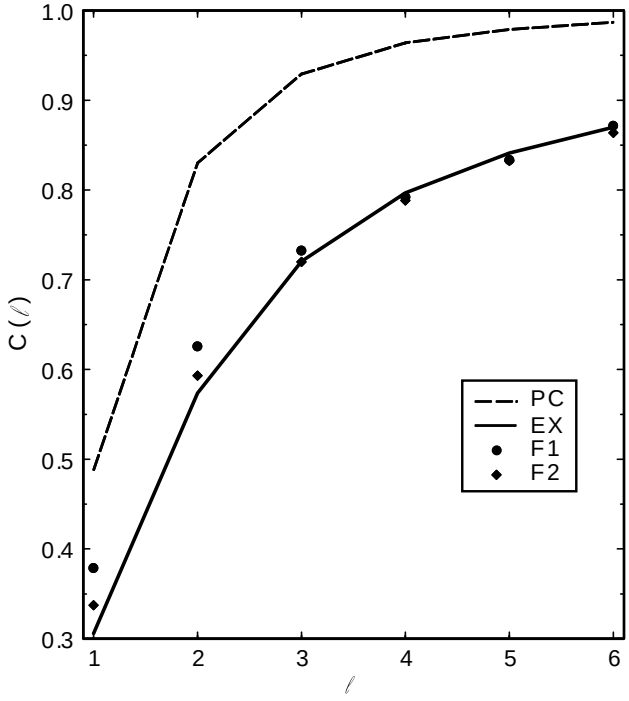

Fig. 1. The correction factors $C(\ell)$ are plotted against ℓ. The dashed line is the estimate based on the point charge Coulomb interaction (eq. (6)). The solid line is calculated from the actual potential. The filled circles and diamonds are the results of the first and second iterations, respectively.

Our first goal is to check the validity of eq. (6) in the case of a finite-size charge density. For this purpose, the Coulomb potential of ^{208}Pb was calculated using the charge density measured in electron scattering [9]. It was then introduced in the Schrödinger equation and solved numerically. The solution yields both the spectrum and the ground-state wave function. Note that the experimental eigenvalues are reproduced to better than 0.1%, which is quite sufficient for the present aims. We take advantage of this good agreement to denote by EX (exact or experimental) any observable calculated by means of this numerical solution.

The exact correction factors $C(\ell)$, obtained by inverting eq. (3), are displayed as a function of ℓ in fig. 1 (denoted by EX). They are compared with the point charge estimates (PC) obtained by inserting the experimental energies in eq. (6). We note a significant difference between EX and PC values which vanishes very slowly as ℓ increases.

In spite of this large difference, the effects on the moments remain between 5–10%, due to the factor $\ell/2(\ell+1)$

Table 1. Parameters of the trial densities ρ_i, $i = 1, 4$.

ρ_1	$\alpha = 0.3741$		
ρ_2	$\alpha = 0.20074$		
ρ_3	$\alpha = 0.2564222$	$\nu = 1.749$	
ρ_4	$B = -0.57849$	$\beta = 0.315846$	$\alpha = 0.447181$

multiplying $C(\ell)$. Furthermore, the quantities used in practice are the k-th roots of the moments, namely

$$\langle r^k \rangle^{1/k} \quad ,$$

further denoted as r-moments for a short-hand notation. For these quantities, the difference between the estimates based on the two $C(\ell)$-factors is only of about 1–2%. This is sufficient at a qualitative level. However, it is possible to achieve more accurate results by means of iterations; the actual procedure and the convergence of the method will be discussed in the next section.

We conclude this section with the following remark. Starting with the $1p$-$1s$ transition, the series of recurrence relations gives access to moments of the ground-state density with $k \geq 2$. In other words, the method determines mostly the outer part of the wave function. On the other hand, the inner part is very important for the reconstruction of the potential at short distances. In fact, the moment $\langle r^{-2} \rangle$ can also be obtained from the spectrum. Taking the angular momentum ℓ as a parameter, the Hellmann-Feynman [10,11] theorem yields

$$\langle r^{-2} \rangle = \lim_{\ell \to 0} \frac{2\mu}{\hbar^2} \frac{\partial E_\ell}{\partial \ell} \; . \tag{7}$$

Here, the E_ℓ values are given by the energies of the *yrast* line. The delicate point lies in the estimate of the derivative near $\ell = 0$ on the basis of finite differences. From a polynomial fit to the measured levels, we found $\langle r^{-2} \rangle^{-1/2} = 4.62\,\mathrm{fm}$, whereas the exact value is 4.82 fm. This means that eq. (7) does not determine $\langle r^{-2} \rangle^{-1/2}$ to better than 4–5%, but can be regarded as a lower limit.

3 Spectral analysis of muonic ^{208}Pb

Energies of μ-levels in ^{208}Pb, measured up to the $1g_{9/2}$ state [5], yield ground-state density moments up to $\langle r^8 \rangle$. For higher states, the energies are in excellent agreement with the Coulomb point charge values. It is thus possible to get, in principle, much higher moments. However, it is sufficient for our purpose to add the $1h$ and $1i$ levels, limiting us to the moment of order 12.

The determination of the ground-state density from the moments faces a problem similar to the one encountered, for instance, in electron scattering [12]. A sufficiently large functional space has to be generated and this is particularly important for the discussion of the uniqueness of the results, as well as of the amount of uncertainty due to the finite number of determined moments.

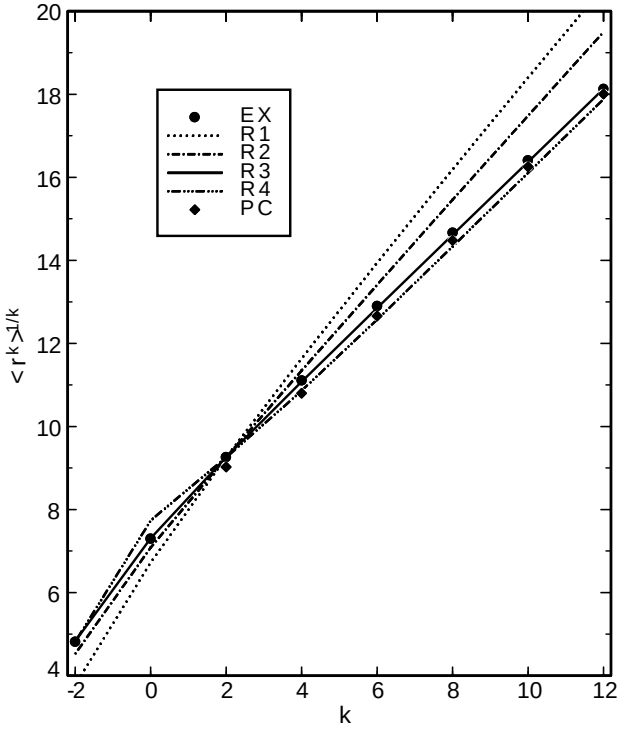

Fig. 2. r-moments (in fm) of the ground-state density. The lines R_1, ..., R_4 show the values of the trial densities ρ_1, ..., ρ_4. The filled circles are the exact values, while the filled diamonds are the estimates of the recurrence relationships (3) with the Coulomb point charge correction factors (6).

The present analysis is less ambitious. Our aim is to explore the potentialities and limitations of the approach. Therefore, we content ourselves with a reasonable trial function. To compare the merits of few possible functions, we first consider the four following densities:

$$\begin{aligned}
R_1 : &\qquad \rho_1(r) = \rho_{01} e^{-\alpha r}, \\
R_2 : &\qquad \rho_2(r) = \rho_{02} [\cosh \alpha r]^{-2}, \\
R_3 : &\qquad \rho_3(r) = \rho_{03} [1 + \cosh \alpha r]^{-\nu}, \\
R_4 : &\qquad \rho_4(r) = \rho_{04} [B e^{-\beta^2 r^2} + e^{-\alpha r}] \, .
\end{aligned}$$

The densities 1, 2 and 4 allow analytical expressions for their moments, while the third one requires a numerical integration. The parameters were determined by a fit to the exact r-moments: $\rho_1(r)$ and $\rho_2(r)$ were fitted to the rms radius ($k = 2$), for $\rho_3(r)$ the fit was made to the rms radius and the r-moment of order 12, and for $\rho_4(r)$ the best overall fit was considered.

The values of the parameters are summarized in table 1. The corresponding r-moments are displayed in fig. 2. They are compared to the exact values EX. Whereas the slopes produced by ρ_1 and ρ_2 readily disqualify these densities, the two other forms are quite acceptable. The fourth density is presented here merely in order to illustrate the question of the non-uniqueness. From its parameters it follows that this density is non-monotonic. It is known from general properties of the Schrödinger equation that the $1s$ wave function has only a single inflection point unless the

Table 2. Eigenvalues (in MeV) of the potentials SF and F1, without and with a Coulomb tail adjusted at 25 fm, compared with the exact values EX.

	SF	F1	SF + Coul	F1 + Coul	EX
$1s$	−10.4967	−10.4967	−10.4966	−10.4965	−10.4975
$1p$	−4.3217	−4.3770	−4.3011	−4.3583	−4.5416
$1d$	−2.3679	−2.0369	−2.0292	−2.0867	−2.0996
$1f$	−1.8842	−0.8566	−1.1777	−1.1827	−1.1816
$1g$	−1.6220	−0.0096	−0.7561	−0.7563	−0.7562
$2s$	−3.5246	−3.5275	−3.3949	−3.5151	−3.4843
$3s$	−2.2967	−1.3445	−1.6849	−1.7157	−1.7088
$4s$	−1.6223	−0.0138	−1.0012	−1.0133	−1.0108
$5s$	−0.6927	+1.0975	−0.6389	−0.6465	−0.6670

Table 3. Eigenvalues (in MeV) of the potentials F1, F2, and BF with a Coulomb tail beyond 25 fm. They are compared with the exact values EX.

	F1	F2	BF	EX
$1s$	−10.4965	−10.4966	−10.4966	−10.4975
$1p$	−4.3583	−4.4701	−4.5500	−4.5416
$1d$	−2.0867	−2.1003	−2.1132	−2.0996
$1f$	−1.1827	−1.1832	−1.1837	−1.1816
$1g$	−0.7563	−0.7563	−0.7563	−0.7562
$2s$	−3.5151	−3.5073	−3.5051	−3.4843
$3s$	−1.7157	−1.7129	−1.7118	−1.7088
$4s$	−1.0133	−1.0120	−1.0114	−1.0108
$5s$	−0.6465	−0.6456	−0.6452	−0.6670

potential has a strongly non-monotonic radial dependence. We expect *a priori* a smooth behaviour of the potential in our case but this assumption can be verified *a posteriori*. For this reason, the form 4 has to be rejected from the set of possible trial functions. For the sake of comparison, we also display in fig. 2 the r-moments obtained from (3) with the point charge values of $C(\ell)$ (denoted by PC). Note that the differences between the EX and PC r-moments is of the order of 2% for $k = 2$ and about 1% for $k = 12$. On the other hand, if the correction factor is simply ignored ($C(\ell) = 0$), a systematic overestimate of 4% is observed.

In view of the above results we adopted the following trial function:

$$\rho(r) = \rho_0 \left[B + \cosh\left(\alpha r + \beta r^{3/2}\right)\right]^{-\nu} . \tag{8}$$

The parameter B influences the behaviour near the origin. In this respect a better estimate of $\langle r^{-2}\rangle$ would be highly desirable. A small amount of $r^{3/2}$ in the cosh improves the curvature around the point of steepest slope. However, this term produces an asymptotic behaviour of the corresponding potential which does not agree with the Coulomb interaction. It means that this choice may have undesirable features at large distances.

With the trial density (8), we start the iterative procedure. Note that the search for the B and β parameters is done (roughly) at the beginning, whereas α and ν result from careful fits. In the first step, we consider the r-moments given by eq. (3) with the point charge $C(\ell)$. Fitting the $k = 2$ and 12 values, we obtain the two following parametrizations:

SF: $B=0$, $\beta=0$, $\alpha=0.2885892$, $\nu=1.5467$,
F1: $B=1.5$, $\beta=0.01$, $\alpha=0.39044886$, $\nu=0.953968$.

Note that SF corresponds to ρ_3; we keep it for the sake of comparison. The r-moments given by these two densities are essentially the ones denoted by PC in fig. 2. Consequently, we learn little from these values (except a qualitative overall agreement). In order to get a deeper

Table 4. r-moments (in fm) of the densities SF, F1, F2, and BF compared with the exact values EX.

	SF	F1	F2	BF	EX
−2	4.6492	4.6046	4.7309	4.8017	4.8178
0	7.0831	7.0472	7.1903	7.2840	7.2988
2	9.0275	9.0275	9.1653	9.2583	9.2585
4	10.8586	10.9010	11.0250	11.1116	11.1060
6	12.6565	12.7269	12.8354	12.9141	12.9017
8	14.4436	14.5170	14.6109	14.6819	14.6656
10	16.2253	16.2746	16.3551	16.4191	16.4059
12	18.0021	18.0021	18.0701	18.1275	18.1276

insight, it is better to look at the corresponding potentials, which are obtained by inverting the Schrödinger equation

$$V(r) = E_{1s} + \frac{\hbar^2}{2\,\mu}\left[\frac{\Phi''_{1s}}{\Phi_{1s}} + \frac{2}{r}\frac{\Phi'_{1s}}{\Phi_{1s}}\right] . \tag{9}$$

Here, the prime and double prime denote the first and second derivative with respect to r, respectively. The ground-state wave function is obtained by taking the square root of the density. The two potentials are then introduced into the Schrödinger equation, which is solved numerically. By comparing the eigenvalues calculated with the SF and F1 potentials with the exact ones, we find that they both fail to reproduce the actual spectrum. From table 2, we see that SF has a tendency of overbinding, apart from the $1p$-level, while F1 yields systematically underbound values. In particular, the $\ell = 5$ and 6 states are unbound. In both cases, these effects are due to the asymptotic forms. It is clear that a simple trial function is not expected to match the exact solution on the entire space.

To remedy this defect and pursue the iterative procedure, it is necessary to cut the parametrized potential at a certain radius and to match it with a Coulomb tail. A radius of 25 fm was chosen. At such a distance, the finite extension of the nuclear charge density has no influence. In general, the shape of the tail is a delicate problem, the

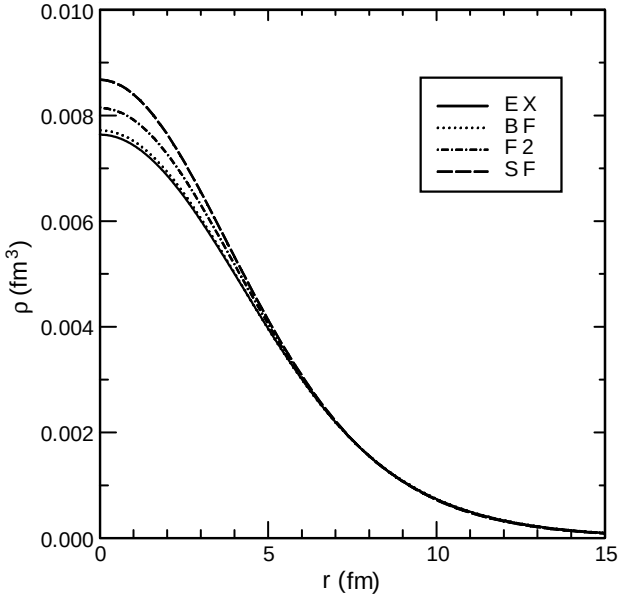

Fig. 3. The densities of the SF, F2 and BF parametrizations are compared with the exact value.

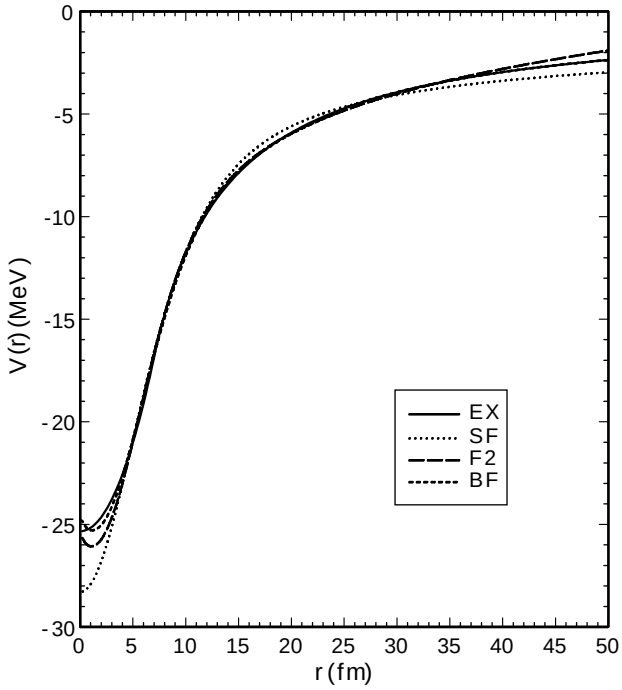

Fig. 4. The potentials obtained from the SF, F2 and BF parametrizations are compared with the actual (EX) potential.

choice being non-unique. In the case of Coulomb systems, however, we are guided by the fact that the highest part of the spectrum is well reproduced by the $1/r$-potential, which greatly simplifies the search.

The results are summarized in table 2. The Coulomb tail in both cases brings the higher levels to their exact values, with little effect on the lower energies. The F1 + Coul parametrization produces somewhat better energies than SF + Coul, as expected from enlarging the parameter space.

At this stage, the crucial test for the iterative procedure is the use of the potential F1 with the adjusted Coulomb tail in the calculation of a new approximation of $C(\ell)$. Note that we have verified that in the absence of the Coulomb tail, it was not possible to get estimates of the correction factors beyond $\ell = 1$ or 2. The results denoted as F1 are displayed in fig. 1. The improvement over the point charge values is appreciable and suggests that the procedure has a good chance to converge.

In the next step, the new correction factors $C(\ell)$ were used in eq. (3), together with the experimental energies, in order to obtain the second approximate set of r-moments. These moments lie roughly in between those of the first approximation and the exact ones. Fitting the new values for $k = 2$ and 12 with the trial density (8) yields the following parameters:

$$\text{F2:}\quad B=1.5,\quad \beta=0.01,\quad \alpha=0.3597609,\quad \nu=1.02239.$$

The corresponding potential F2 is again introduced in the Schrödinger equation. Without the Coulomb tail, the potential F2 has the same tendency as F1 to underbind the levels, particularly beyond $\ell = 3$. Consequently, fitting the Coulomb tail is again required in order to achieve a good agreement with the higher part of the spectrum and calculate the next approximation to $C(\ell)$. Eigenvalues and r-moments will be discussed below. As far as $C(\ell)$ is concerned, the results denoted as F2 are displayed in fig. 1. Whereas the convergence is quite satisfactory for $\ell \geq 2$, it is rather slow for $\ell = 1$. We have verified that in the third iteration, F3 produces the value of $C(1)$ which is still 5% away from the exact number. In fact, about 10 iterations are required to reach the convergence. However, it is not our purpose to pursue the iterative procedure further. First, we have already at this stage a good understanding of the ability and limitations of the approach. Secondly, we are dealing with a specific trial density containing a limited number of parameters. Thus the trial functional space is too small to ensure the convergence towards the exact form. On the other hand, we may partially estimate the efficiency of the trial density and get a feeling of the final results by fitting the exact r-moments. We here implicitly assume that the iterations converge towards the exact $C(\ell)$, which is well supported by the results displayed in fig. 1. This final parametrization has the following parameters:

$$\text{BF:}\quad B=1.5,\quad \beta=0.01,\quad \alpha=0.34271794,\quad \nu=1.063933.$$

As before, the corresponding potential is calculated by means of eq. (9) and a Coulombic tail is matched beyond 25 fm. This potential is introduced in the Schrödinger equation to obtain the eigenvalues.

To summarize our results, we first display in table 3 eigenvalues corresponding to F1, F2 and BF potentials, with a Coulomb tail adjusted at 25 fm compared to the exact values. The improvement of F2 over F1 is clear for the lower states. It is interesting to note that the iterations are converging towards the BF results rather than

to the exact values. The differences between BF and the latter indicate a slight systematic overbinding, except for the higher s-levels. The deviation is 0.8% for $\ell = 1$ and decreases to 0.2% for $\ell = 3$. The deviation for the $2s$ state reaches 0.6%. It clearly establishes the limits of the trial density and the accuracy we can expect.

Results for the r-moments are collected in table 4 for SF, F1, F2 and BF parametrizations and compared with the exact values. Remember that SF and F1 fit moments obtained with the point charge estimate of $C(\ell)$, whereas F2 relies on the first iteration (see fig. 1). We also quote values for $k = -2$ and 0, although their exact values EX are calculated and not derived from the spectrum. Note that for $k = 0$, the r-moment is defined as the limit

$$\lim_{k\to\ 0} \langle r^k \rangle^{1/k} = \exp\left(\int_0^\infty \rho(r)\, r^2 \ln r \, \mathrm{d}r \right) . \qquad (10)$$

It is interesting to note the slow convergence towards the moments of BF as the correction factors get closer to the exact values. On the other hand, BF produces intermediate r-moments slightly larger than the exact ones. The differences are of the order of 0.1%. As in the case of the energies, this fixes the accuracy which can be reached with the simple trial density (8).

In fig. 3, we display the densities of the parametrizations SF, F2 and BF compared to the exact density. The improvement is remarkable particularly near the origin. This clearly underlines the importance of determining $\langle r^{-2} \rangle^{-1/2}$ to an accuracy better than 1%.

Finally, the potentials corresponding to SF, F2 and BF are displayed in fig. 4 and compared to the exact values EX. Apart from SF, there is a remarkable agreement with the actual potential over the intermediate range $3 \leq r \leq 25$ fm and the agreement extends to at least 50 fm for BF. This gives us confidence in the use of an adjusted tail to ensure the convergence of the iterations. As for the densities, the most controversial place arises near the origin. There, we observe a non-monotonic behaviour for the potentials F2 and BF. It is related to the presence of the $r^{3/2}$ term in the cosh. Contrarily to the problem of the tail, which is solved by considering general properties of the Coulomb interaction, uncertainties around the origin are more difficult to tackle. The argument advocated to reject non-monotonic densities does not apply to potentials.

4 Conclusions

We have applied to the ^{208}Pb muonic atom the series of recurrence relations connecting the moments of the ground-state density to the energy differences between the $1s$ level and the states of the *yrast* line. The large amount of precise experimental data, and the Coulombic higher part of the spectrum allowed a detailed test of the method for determining the ground-state density. The next step, reconstructing the local equivalent potential, has also been investigated. In this respect, the electromagnetic character of the interaction has greatly facilitated the interpretation of the results.

The present investigation is not exhaustive; we have merely restricted ourselves to the study of the efficiency of a given trial density. In spite of this limitation, the present work clearly underlines the possibilities of the method, as well as the difficulties one would face in a more thorough and systematic approach.

At a qualitative level, the method is straightforward, provided a reasonable trial density is used. A semi-quantitative attempt requires an iterative procedure, particularly in order to determine the correction factors $C(\ell)$ with sufficient accuracy. In this respect, the solution of the Schrödinger equation, with the approximate and the iterated potentials, plays a key role. The comparison between the calculated spectrum and the measured energies at each step is a valuable source of information.

The present analysis achieves an accuracy better than 1% on the ground-state moments and density. The potential is also well reproduced, except near the origin and in the far tail. To achieve higher accuracy, more elaborate techniques are required for the determination of the density from its moments. Nevertheless, the present results are very encouraging, and application to less known systems is planned. This is the case of hadronic atoms [13] where, in addition to the electromagnetic interaction, the strong interaction is involved.

Reconstructing the potential, the present method has features similar to the ones encountered in the inversion technique based on the phase shifts. Careful studies have shown that in many cases the intermediate range is relatively well obtained, whereas instabilities appear near the origin and in the tail [14]. On the other hand, the present results shed some light on the more usual method, which consists in fitting the spectrum by means of a parametrized potential. It shows that among all the levels, the *yrast* line plays a key role. Furthermore as the number of fitted levels along this line increases, the solution tends to become unique if the functional space describing the potential is sufficiently large. These two last remarks were certainly already known, at least empirically, but the connection between the ground-state moments and the *yrast* levels yields a formal support.

This research was partially supported by the Grant Agency of the Czech Republic (J.M., grant No. 202/00/1667). J.M. acknowledges the hospitality of the Group of Theoretical Physics, IPN Orsay.

References

1. R.J. Lombard, J. Mareš, Phys. Rev. C **52**, 170 (1995).
2. F.-Z. Ighezou, R.J. Lombard, Ann. Phys. (N.Y.) **278**, 265 (1999).
3. R.A. Bertlmann, A. Martin, Nucl. Phys. B **168**, 111 (1980); **182**, 35 (1981).
4. R.J. Lombard, S. Marcos, J. Mareš, Phys. Rev. C **50**, 2900 (1994).
5. R. Engfer, H. Schneuwly, J.L. Vuilleumier, H.K. Walter, A. Zehnder, At. Data Nucl. Data Tables **14**, 509 (1974).
6. R.C. Barrett, D.F. Jackson, *Nuclear Sizes and Structure* (Clarendon Press, Oxford, 1977).

7. See, for instance, K. Chadan, P.C. Sabatier, *Inverse Problem in Quantum Scattering Theory*, 2nd edition (Springer-Verlag, New York, 1989).
8. R.J. Lombard, J. Mareš, Phys. Rev. D **59**, 076005 (1999).
9. B. Frois *et al.*, Phys. Rev. Lett. **38**, 38 (1977).
10. G. Hellmann, *Einführung in die Quantumchemie* (F. Denticke, Leipzig and Vienna, 1937).
11. R.P. Feynman, Phys. Rev. **56**, 340 (1939).
12. J. Friedrich, F. Lenz, Nucl. Phys. A **183**, 523 (1972).
13. C.J. Batty, E. Friedman, A. Gal, Phys. Rep. **287**, 385 (1997).
14. C. Coudray, *Quelques aspects du problème inverse de la diffusion à énergie fixée*, Thèse, Orsay, No. 2160 (1979).